

PRODUCTION OF VECTOR MESONS IN $pp \rightarrow pVp$ REACTIONS WITH ELECTROMAGNETIC DISSOCIATION OF PROTONS*

ANNA CISEK^a, WOLFGANG SCHÄFER^b, ANTONI SZCZUREK^{a,b}

^aCollege of Natural Sciences, Institute of Physics, University of Rzeszów
Pigonia 1, 35-310 Rzeszów, Poland

^bInstitute of Nuclear Physics Polish Academy of Sciences
Radzikowskiego 152, 31-342 Kraków, Poland

(Received May 18, 2020)

We discuss the semi-exclusive production of vector mesons in proton–proton collisions with electromagnetic dissociation of one of the protons. Several differential distribution in missing mass (M_X) or single-particle variables related exclusively to the produced vector meson are calculated for the pp center-of-mass energies of 7 and 13 TeV. The cross sections and some differential distributions are compared to their counterparts for purely exclusive reaction $pp \rightarrow pVp$. For electromagnetic dissociation, the important property is that the $p\gamma^* \rightarrow Xp$ transitions are given by the electromagnetic structure function of proton. In our calculations, we use different parametrizations of the structure function and discuss how it is constrained by the data on virtual photoabsorption on a proton.

DOI:10.5506/APhysPolB.51.1305

1. Introduction

Exclusive production of vector mesons $pp \rightarrow ppV$ is a source of information on the small- x gluon distributions in the proton. In the k_t -factorization approach, the cross section depends not only on unintegrated gluon distribution function (UGDF) but also on the wave function of the vector meson [1]. It was shown that the exclusive cross section is very sensitive to the choice of the UGDF.

So far, both (almost) exclusive J/ψ and Υ production [2, 3] were measured in proton–proton collisions at the LHC. The measurements are not fully exclusive because the outgoing protons were not measured, but only

* Presented at XXVI Cracow Epiphany Conference on LHC Physics: Standard Model and Beyond, Kraków, Poland, January 7–10, 2020.

a veto on particle production in a large rapidity interval was imposed. For proton–proton collisions, two types of proton excitations are possible: diffractive and electromagnetic. In our earlier paper on J/ψ production [4], we have developed a formalism how to calculate processes with rapidity gaps, but including proton dissociation. To calculate electromagnetic dissociation, the method uses parametrizations of the proton structure functions which are used to derive an inelastic photon flux. We have shown in [4] that the semi-exclusive mechanism cannot be completely removed by the rapidity veto on additional produced particles. We were a bit surprised that the electromagnetic dissociation seems the most important. Here, we wish to show more systematic studies for production of different vector mesons and better understand the competition of the purely exclusive and the semi-exclusive processes.

The semi-exclusive production of vector mesons in proton–proton collisions with electromagnetic dissociation of protons is illustrated in Fig. 1.

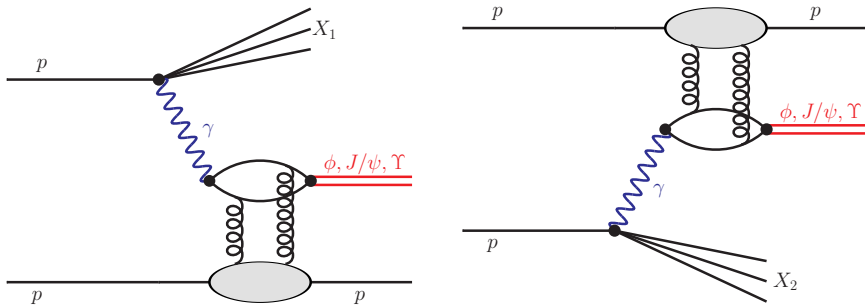


Fig. 1. Schematic representation of the electromagnetic excitation of first (left panel) or second (right panel) proton.

Here, we review our calculations of different differential distributions. We are especially interested in the ratio of the semi-exclusive to exclusive cross section. Such a ratio may be considered as a measure of “unwanted” contamination of exclusive processes when using the rapidity gap method.

2. Formalism for semi-exclusive production of vector meson with electromagnetic dissociation

The important property of these processes is that the $p\gamma^* \rightarrow X$ transition is given by the electromagnetic structure functions of the proton, and thus to a large extent calculable “from data”, using parametrizations of these

structure functions. The cross section for such processes can be written as

$$\begin{aligned} & \frac{d\sigma(pp \rightarrow XVp; s)}{dy d^2\mathbf{p} dM_X^2} \\ &= \int \frac{d^2\mathbf{q}}{\pi q^2} \mathcal{F}_{\gamma/p}^{(\text{inel})}(z_+, \mathbf{q}^2, M_X^2) \frac{1}{\pi} \frac{d\sigma^{\gamma^* p \rightarrow Vp}}{dt}(z_+, s, t = -(\mathbf{q} - \mathbf{p})^2) \\ &+ (z_+ \leftrightarrow z_-), \end{aligned} \tag{1}$$

where $z_{\pm} = e^{\pm y} \sqrt{(\mathbf{p}^2 + m_V^2)}/s$ is the fraction of the proton's longitudinal momentum carried by the photon, M_X is the invariant mass of the excited system X , \mathbf{p} is the transverse momentum of the vector meson, and $-\mathbf{q}$ is the transverse momentum of the outgoing hadronic system X . Below we also use $p_t = |\mathbf{p}|$ for the absolute value of the transverse momentum. The mass of the excited hadronic system must be above the threshold $M_{\text{thr}} = m_{\pi} + m_p$.

We can calculate the “fully unintegrated” flux of photons associated with the breakup of the proton in terms of the structure function F_2 of a proton

$$\begin{aligned} \mathcal{F}_{\gamma/p}^{(\text{inel})}(z, \mathbf{q}^2, M_X^2) &= \frac{\alpha_{\text{em}}}{\pi} (1-z) \theta(M_X^2 - M_{\text{thr}}^2) \frac{F_2(x_{\text{Bj}}, Q^2)}{M_X^2 + Q^2 - m_p^2} \\ &\times \left[\frac{\mathbf{q}^2}{\mathbf{q}^2 + z(M_X^2 - m_p^2) + z^2 m_p^2} \right]^2, \end{aligned} \tag{2}$$

where the photon virtuality Q^2 and the Bjorken variable x_{Bj} are obtained from

$$Q^2 = \frac{1}{1-z} [\mathbf{q}^2 + z(M_X^2 - m_p^2) + z^2 m_p^2], \quad x_{\text{Bj}} = \frac{Q^2}{Q^2 + M_X^2 - m_p^2}. \tag{3}$$

We used a number of parametrizations of the proton structure function $F_2(x, Q^2)$ from the literature [5]:

1. A parametrization of Refs. [6, 7] which is fitted to the lower energy CLAS data and is meant to give an accurate description especially in the resonance region. In the figures, it will be labeled FFJLM. Therefore, we used this parameterization when calculating observables $M_X \lesssim 2$ GeV.
2. The Abramowicz–Levy–Levin–Maor fit [8, 9] used previously also in [10], abbreviated here ALLM.
3. A newly constructed parametrization, which at $Q^2 > 9$ GeV² uses an NNLO calculation of F_2 and F_L from NNLO MSTW 2008 partons [11].

This fit uses the parametrization of Bosted and Christy [12] in the resonance region, and a version of the ALLM fit published by the HERMES Collaboration [13] for the continuum region. It also uses information on the longitudinal structure function from SLAC [14]. As the fit is constructed closely following the LUXqed work of Refs. [15, 16], we call this fit LUX in the figures.

4. A Vector-Meson-Dominance model (VDM) inspired fit of F_2 proposed in [17] at low Q^2 , which is completed by the same NNLO MSTW structure function as above at large Q^2 . This fit is labeled SU for brevity.

3. Results

In Figs. 2 and 3, we show the rapidity distribution for semi-exclusive production of vector mesons for the proton–proton collision energies of 7 TeV (Fig. 2) and 13 TeV (Fig. 3). In the left panel, we present our results for the ϕ meson, in the middle panel for the J/ψ meson, and in the right panel for the Υ meson. We show the results for different parametrizations of the F_2 structure function. The solid blue lines are for Abramowicz–Levin–Levy–Maor (ALLM) [8], the dash-dotted red lines are for Fiore–Flachi–Jenkowszky–Lengyel–Magas (FFJLM) [7], the dashed green lines are for Szczurek–Uleshchenko (SU) [17] fits to F_2 and the dotted lines are for the VDM contribution alone.

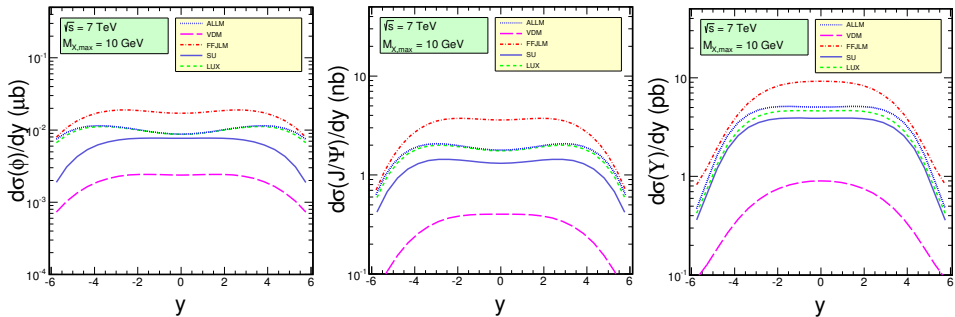


Fig. 2. (Color online) Rapidity distribution for pp cm-energy $\sqrt{s} = 7$ TeV for the production of ϕ , J/ψ and Υ mesons for different parametrizations of the proton structure function F_2 .

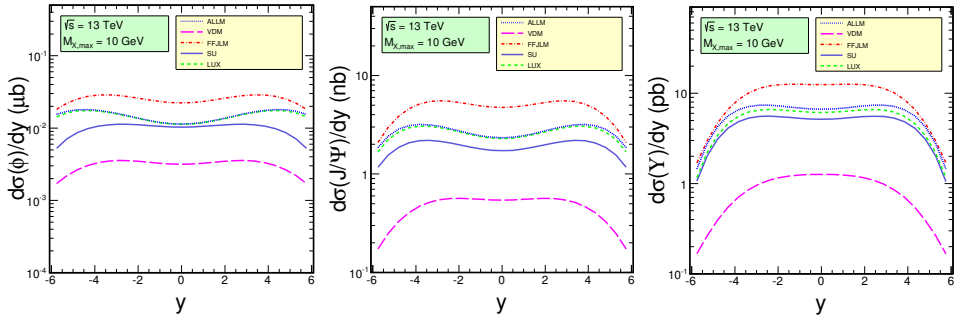


Fig. 3. (Color online) Rapidity distribution for pp cm-energy $\sqrt{s} = 13$ TeV for the production of ϕ , J/ψ and Υ mesons for different parametrizations of the proton structure function F_2 .

In Figs. 4 and 5, we show the transverse momentum distribution for semi-exclusive production of vector mesons for the energies 7 TeV (Fig. 4) and 13 TeV (Fig. 5). Again, in the left panel, we presents results for the ϕ meson, in the middle panel for the J/ψ meson, and in the right panel for the Υ meson, using different parametrizations of the F_2 structure function. The notation of lines are the same as in Fig. 2.

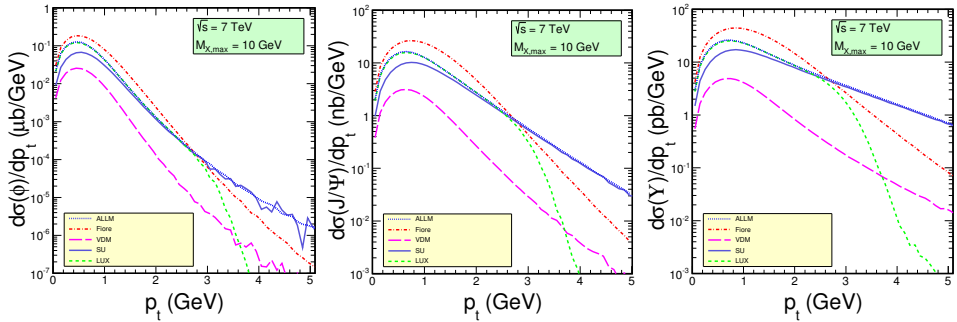


Fig. 4. (Color online) Transverse momentum distribution of vector meson for pp cm-energy $\sqrt{s} = 7$ TeV for the production of ϕ , J/ψ and Υ mesons for different parametrizations of the proton structure function F_2 .

The results presented in Figs. 2–5 are for the missing mass $M_X < 10$ GeV. Note that the FFJLM parametrization is reasonable only for $M_X < 2$ GeV, while the ALLM parametrization works well in a much broader range of missing masses M_X , but does not have explicit resonance contributions.

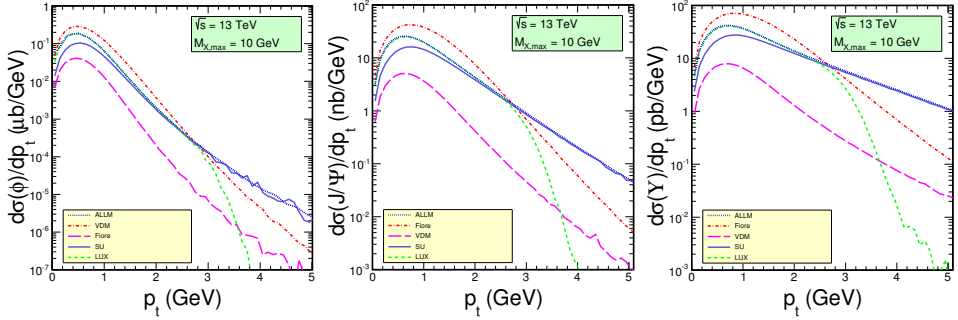


Fig. 5. (Color online) Transverse momentum distribution of vector meson for pp cm-energy $\sqrt{s} = 13$ TeV for the production of ϕ , J/ψ and Υ mesons for different parametrizations of the proton structure function F_2 .

In Figs. 6 and 7, we show a comparison of the cross section for the production of vector mesons: ϕ , J/ψ and Υ for energies $\sqrt{s} = 7$ TeV (Fig. 6) and $\sqrt{s} = 13$ TeV (Fig. 7). The presented results are for the missing mass cut $M_X < 10$ GeV. We show results for different parametrizations of the F_2 structure function.

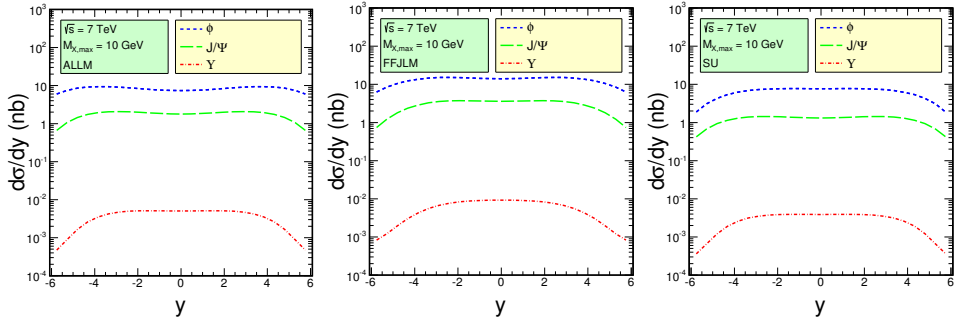


Fig. 6. Rapidity distribution for pp cm-energy $\sqrt{s} = 7$ TeV for the production of ϕ , J/ψ and Υ mesons for different parametrizations of the proton structure function F_2 .

In Figs. 8 and 9, we show the ratio $R^{\text{EM/excl.}}$ as a function of rapidity for different upper limits on missing mass M_X . The ALLM-type structure function of proton was used for these calculations. We show the results for different vector mesons production: ϕ (left), J/ψ (middle) and Υ (right).

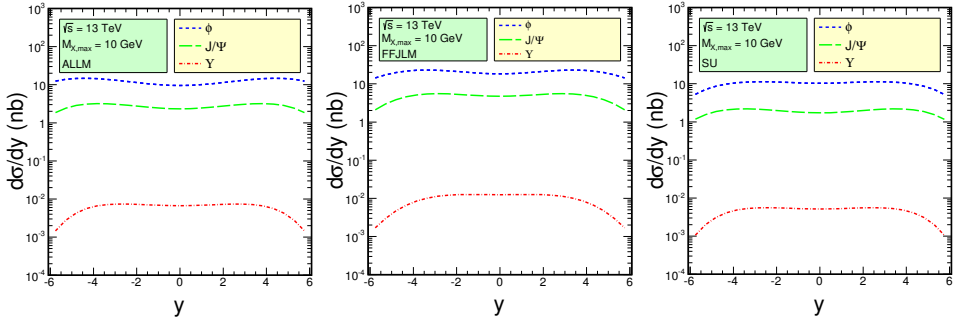


Fig. 7. Rapidity distribution for pp cm-energy $\sqrt{s} = 13$ TeV for the production of ϕ , J/ψ and Υ mesons for different parametrizations of the proton structure function F_2 .

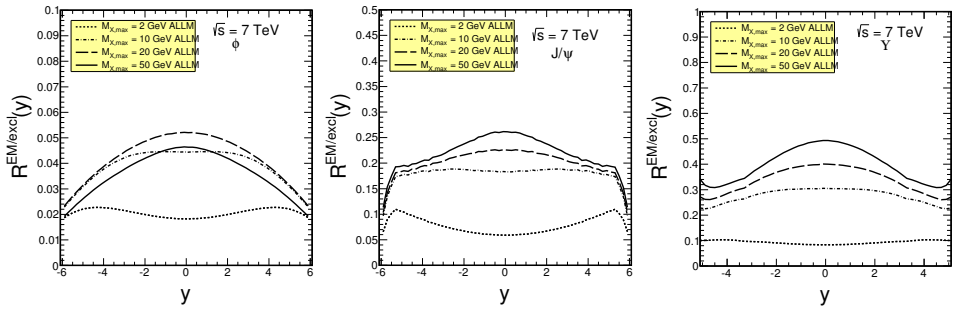


Fig. 8. Ratio of inelastic diffractive to exclusive vector meson production as a function of rapidity for different upper limits on the excited mass M_X and energy $\sqrt{s} = 7$ TeV.

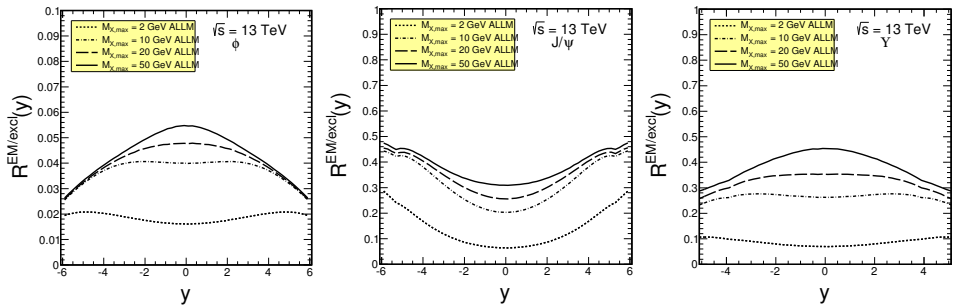


Fig. 9. Ratio of inelastic diffractive to exclusive vector meson production as a function of rapidity for different upper limits on the excited mass M_X and energy $\sqrt{s} = 13$ TeV.

In Figs. 10 and 11, we show the ratio $R^{\text{EM/excl}}$ as a function of transverse momentum for different upper limits on M_X . We see that as soon as high mass states are included, the inelastic contribution dominates at $p_t \gtrsim 1$ GeV.

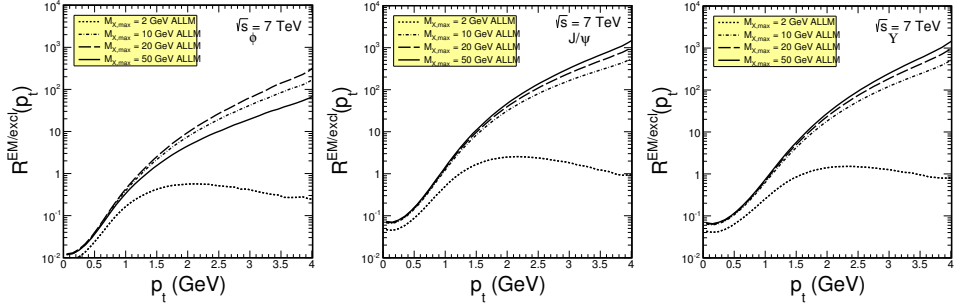


Fig. 10. Ratio of inelastic diffractive to exclusive vector meson production as a function of transverse momentum or different upper limits on the excited mass M_X and energy $\sqrt{s} = 7$ TeV.

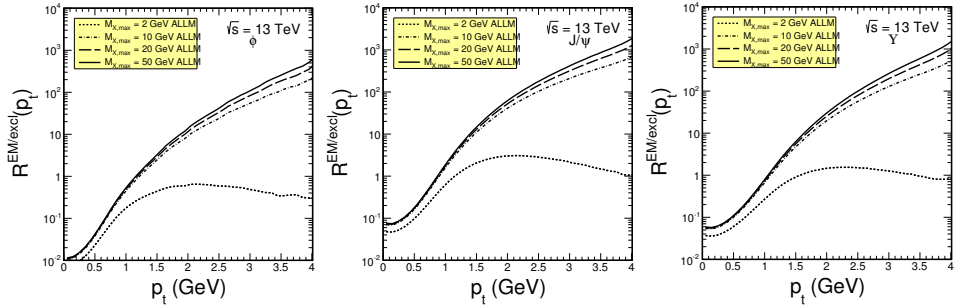


Fig. 11. Ratio of inelastic diffractive to exclusive vector meson production as a function of transverse momentum or different upper limits on the excited mass M_X and energy $\sqrt{s} = 13$ TeV.

In Figs. 12 and 13, we show the sums of the two single-proton excitations. The presented results are for energy of 7 TeV and different cuts on the maximal missing mass. In the left panel, we show results for $M_X < 2$ GeV, in the middle panel for $M_X < 5$ GeV, and in the right panel for $M_X < 10$ GeV. We show the contribution of low-mass electromagnetic excitation with FFJLM (dotted line) and ALLM (dashed line) parametrizations of the F_2 structure functions. Similarly, we show the contributions of the diffractive partonic mechanism (short-dashed line) and of resonances (dash-dotted line) [4]. For comparison, we show also the contribution of the purely exclusive process $pp \rightarrow pJ/\psi p$ (top solid line) [1]. We predict that the contribution of low

mass excitations gives camel-like shapes with maxima at $y \approx \pm 4$. When higher (nonresonant) mass region is included the semiexclusive cross section grows considerably and the two separated maxima merge into one maximum at $y = 0$.

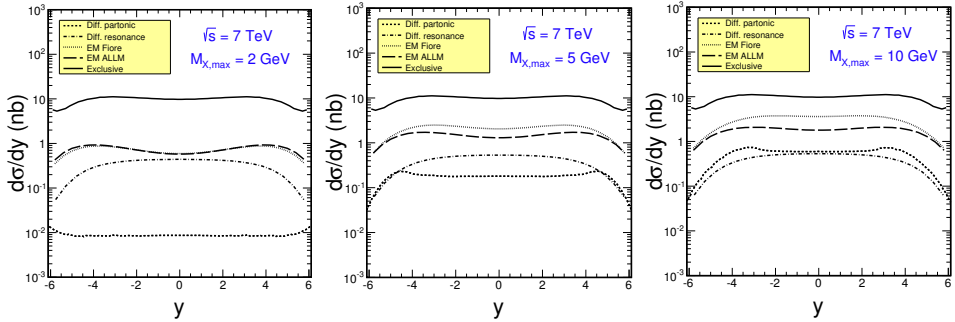


Fig. 12. Rapidity distribution of J/ψ mesons produced at $\sqrt{s} = 7$ TeV energy when one of the protons is excited due to photon or Pomeron exchange. Both contributions (one or second proton excitation) are added together. We also show a reference distribution for the $pp \rightarrow pJ/\psi p$ exclusive process with parameters taken from [1].

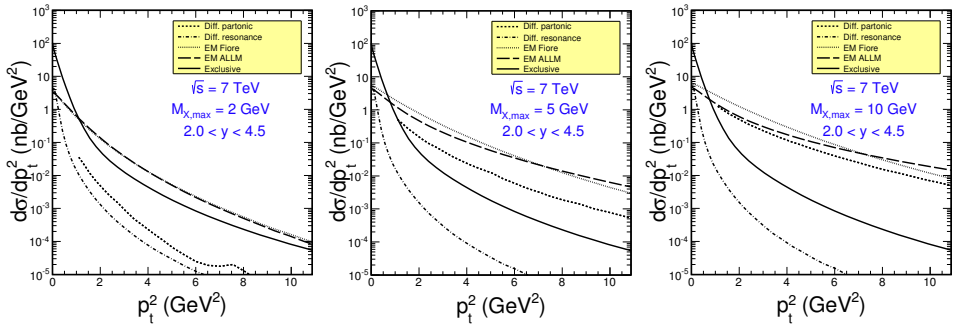


Fig. 13. Transverse momentum distribution of J/ψ mesons at $\sqrt{s} = 7$ TeV energy. Shown are the cross sections when one of the protons is excited (due to photon or Pomeron exchange). We also show a reference distribution for the $pp \rightarrow pJ/\psi p$ from [1].

4. Conclusions

In this paper, we have discussed semi-exclusive production of vector mesons in $pp \rightarrow VpX$ processes, where X stands for excited/dissociated proton system and $V = \phi, J/\psi, \Upsilon$. These results were obtained in our recent papers [4, 5]. Electromagnetic dissociation of protons is calculated using an inelastic unintegrated photon flux which was calculated based on

modern parametrizations of deep-inelastic proton structure functions. Different parametrizations from the literature have been used. The results strongly depend on the parametrization of the structure function used. In γ -Pomeron fusion reactions in proton-proton scattering, electromagnetic dissociation is of the same size as strong, diffractive dissociation. It even dominates in some regions of the phase space. The ratio of the semi-exclusive to the purely exclusive contributions strongly depends on the vector meson transverse momentum and only mildly on rapidity. In general, the bigger semi-exclusive to exclusive ratio is obtained for heavier quarkonia.

REFERENCES

- [1] A. Cisek, W. Schäfer, A. Szczurek, *J. High Energy Phys.* **1504**, 159 (2015).
- [2] LHCb Collaboration (R. Aaij *et al.*), *J. Phys. G: Nucl. Part. Phys.* **40**, 045001 (2013), [arXiv:1301.7084 \[hep-ex\]](#).
- [3] LHCb Collaboration (R. Aaij *et al.*), *J. High Energy Phys.* **1509**, 084 (2015), [arXiv:1505.08139 \[hep-ex\]](#).
- [4] A. Cisek, W. Schäfer, A. Szczurek, *Phys. Lett. B* **769**, 176 (2017), [arXiv:1611.08210 \[hep-ph\]](#).
- [5] A. Cisek, W. Schäfer, A. Szczurek, *Phys. Rev. D* **100**, 114022 (2019), [arXiv:1910.03264 \[hep-ph\]](#).
- [6] R. Fiore *et al.*, *Eur. Phys. J. A* **15**, 505 (2002), [arXiv:hep-ph/0206027](#).
- [7] R. Fiore, L.L. Jenkovszky, F. Paccanoni, A. Prokudin, *Phys. Rev. D* **70**, 054003 (2004), [arXiv:hep-ph/0404021](#).
- [8] H. Abramowicz, E.M. Levin, A. Levy, U. Maor, *Phys. Lett. B* **269**, 465 (1991).
- [9] H. Abramowicz, A. Levy, [arXiv:hep-ph/9712415](#).
- [10] M. Łuszczak, W. Schäfer, A. Szczurek, *Phys. Rev. D* **93**, 074018 (2016), [arXiv:1510.00294 \[hep-ph\]](#).
- [11] A.D. Martin, W.J. Stirling, R.S. Thorne, G. Watt, *Eur. Phys. J. C* **63**, 189 (2009), [arXiv:0901.0002 \[hep-ph\]](#).
- [12] P.E. Bosted, M.E. Christy, *Phys. Rev. C* **77**, 065206 (2008), [arXiv:0711.0159 \[hep-ph\]](#).
- [13] HERMES Collaboration (A. Airapetian *et al.*), *J. High Energy Phys.* **1105**, 126 (2011), [arXiv:1103.5704 \[hep-ex\]](#).
- [14] E143 Collaboration (K. Abe *et al.*), *Phys. Lett. B* **452**, 194 (1999), [arXiv:hep-ex/9808028](#).
- [15] A. Manohar, P. Nason, G.P. Salam, G. Zanderighi, *Phys. Rev. Lett.* **117**, 242002 (2016), [arXiv:1607.04266 \[hep-ph\]](#).
- [16] A.V. Manohar, P. Nason, G.P. Salam, G. Zanderighi, *J. High Energy Phys.* **1712**, 046 (2017), [arXiv:1708.01256 \[hep-ph\]](#).
- [17] A. Szczurek, V. Uleshchenko, *Eur. Phys. C* **12**, 663 (2000); *Phys. Lett. B* **475**, 120 (2000).